DOI: 10.1002/chem.200601601

Controlling Polymer Properties through Dynamic Metal–Ligand Interactions: Supramolecular Cruciforms Made Easy

Warren W. Gerhardt, Anthony J. Zucchero, Clinton R. South, Uwe H. F. Bunz,* and Marcus Weck*[a]

Abstract: A straightforward methodology towards the supramolecular synthesis of novel organometallic polymers with attractive optical properties is presented. By coordinating bifunctional fluorescent cruciform molecules through ditopic metalated pincer complexes (Pd or Pt), we have synthesized a new class of well-defined coordination polymers that have controllable and tunable physical and photophysical properties. The formation of these new materials by employing metal coordination was monitored by ^{1}H NMR spectroscopy, the association strength of the metal–ligand interaction was measured by isothermal titration calorimetry, the solution polymeric properties were evaluated by viscometry, and the optical properties were measured and observed by fluorescence spectroscopy. The fast and quantitative synthesis of a wide range of prefabricated monomeric cruciform and metalated-pincer-complex components will allow for the rapid generation, growth, and optimization of this new class of functional polymers, which have potential electronic and optical applications.

Keywords: alkyne ligands · cruciforms · materials science · polymers · supramolecular chemistry

Introduction

Conjugated and fluorescent molecules are candidates for integration into electro-optical and light-emitting devices (LEDs) because of their electrical, optical, and redox properties.[1–6] Polymeric-based systems are desirable owing to their good mechanical and film forming properties. Such systems are amenable to solution processing.[7] Supramolecular polymeric systems based on the assembly of monomeric units by using noncovalent interactions add an additional level of control. Such materials have the potential to combine the processability and mechanical properties of a traditional polymeric system without the long-range defects and functional-group intolerance of covalent polymerization methodologies.[8] Self-assembled materials are dynamic systems with reversible interactions that are responsive to environmental stimuli, which allows the polymeric properties to be adjusted for specific applications. Intense research in this area has yielded supramolecular polymeric materials based on conjugated building blocks with novel applications ranging from tissue engineering[9] to electronic applications.[10] Rowan, Weder, and co-workers have used metal–ligand interactions to form supramolecular fluorescent phenylene ethynylene coordination polymers that can be easily processed into films and fibers.[11–14] We have investigated cross-conjugated fluorescent cruciform-shaped molecules as new electro-optical materials owing to their unique properties,[15–21] as well as distyrylbenzene-substituted poly(*para*-phenylene ethynylene)s.[20] More recently, we have reported our preliminary results on the polymerization of cruciforms by using noncovalent strategies (Scheme 1).[22] These investigations were based on the fluorescent cruciform **1**, which is a building block that can be linearly polymerized through simple metal coordination via its terminal pyridyl moieties by means of coordination to the bispalladated pincer complex **2**. The fast and quantitative self-assembly of these building blocks into polymer **1P** can be accomplished by simply mixing the two components under ambient conditions. We confirmed that the self-assembly event had occurred by ^{1}H NMR spectroscopy, and also showed that there was a molecular-weight dependence of **1P** on the feed monomer stoichiometries by using viscometry. Furthermore, we

[a] W. W. Gerhardt, A. J. Zucchero, C. R. South, Prof. U. H. F. Bunz, Prof. M. Weck
School of Chemistry and Biochemistry
Georgia Institute of Technology
Atlanta, Georgia 30332–0400 (USA)
Fax: (+1) 404-894-7452
E-mail: uwe.bunz@chemistry.gatech.edu
marcus.weck@chemistry.gatech.edu

Supporting information for this article is available on the WWW under http://www.chemeurj.org/ or from the author.

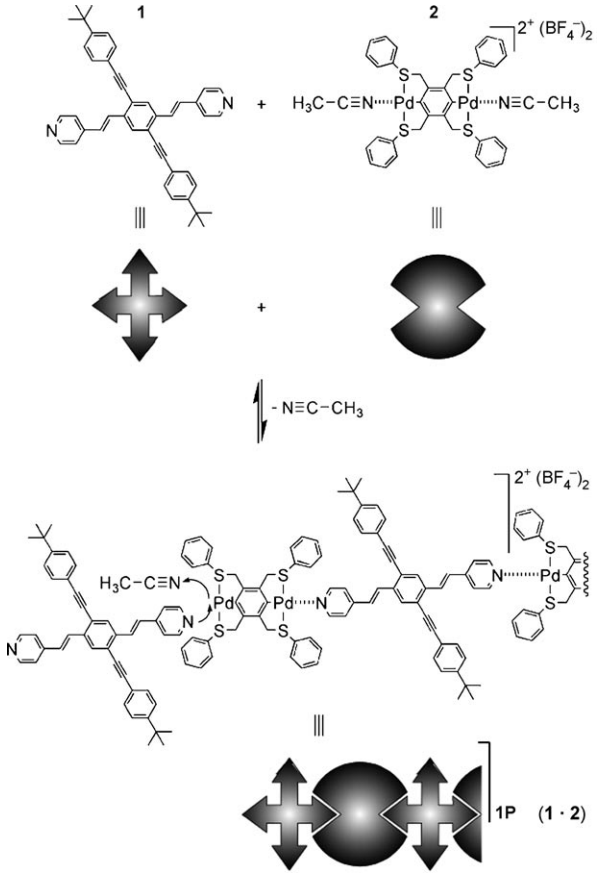

Scheme 1. Coordination polymer **1P**, a fluorescent supramolecular complex with a green emission at 515 nm formed through the coordination of **1** and **2**.

Our toolbox already includes building blocks **1** and **2**. However, we expanded it further by also investigating the self-assembly behavior of pyridyl arylethynylene cruciform **3** and bisplatinated pincer complex **4** (Figure 1). A library of

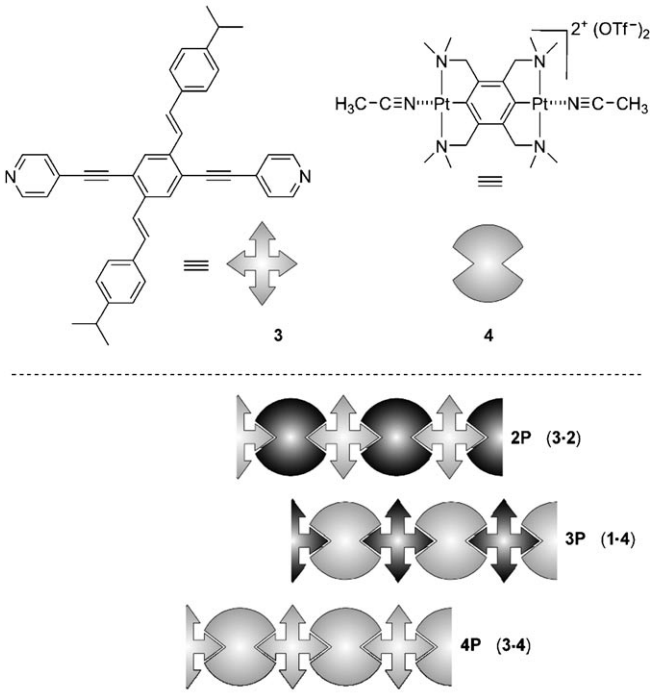

Figure 1. Pyridyl cruciform **3**, bisplatinated pincer complex **4**, and the three supramolecular polymers **2P**–**4P** synthesized from building blocks **1**–**4**.

obtained an association constant (K_a) value of 5700 M^{-1} for **1P** in DMF by using isothermal titration calorimetry (ITC). An approximate value of 14 for the degree of polymerization (DP) was obtained by using the multistage open association (MSOA) model equation.[13,23–25] The resulting functional polymeric material displayed fluorescence, owing to the presence of the small molecule cruciform species within a well-defined supramolecular polymeric framework, and could be solution processed.

Our ultimate goal is to prepare functional and solution-processable materials with physical and optical properties that can be tailored to specific applications. To accomplish this goal, we envisage creating a discrete toolbox of supramolecular monomers that can be polymerized through noncovalent interactions. By readily exchanging monomer components, we can augment the final properties of the materials to fit a specific need by using a simple assembly step, which minimizes or obviates more costly and time consuming synthetic steps. Herein, we report the use of platinum as a new metal center for the coordination event, as well as new cruciforms, which result in polymers with higher K_a values to our palladium-based first-generation material that have controllable physical and optical properties.

related polymers that have a range of physical and optical properties was obtained by coordinating cruciforms through a pyridyl unit, on either the styryl or the arylethynylene axis, to either a bis-Pd or a bis-Pt pincer complex.

The cruciform building blocks that we have investigated (1,4 distyryl-2,5-bisarylethynylbenzene molecules) are part of a larger class of X-shaped molecules with attractive electro-optical properties.[15–19,21,26–33] Haley and co-workers examined tetraarylethynyl substituted cruciforms and reported in-depth luminescence characterizations and self-association studies.[26] The groups of Bunz and Haley have independently demonstrated that donor and acceptor groups placed on separate axial paths lead to molecules in which the frontier molecular orbitals (FMOs) are confined to their respective donor (HOMO) and acceptor (LUMO) substituted arms.[16,17,26]

The other class of building blocks, metalated pincer complexes, are capable of coordinating, both quickly and quantitatively, to a variety of ligands[22,34–46] through strong, single-site, and directional interactions to provide supramolecular architectures. A monoreceptor pincer complex is a tridentate species composed of a central aromatic core that contains a carbon–metal bond (C) flanked by two neutral donor atoms (E), which gives these ligands an ECE nomenclature.

Cyclometalation of these ligands with a Pd or Pt salt creates a square-planar complex, which can coordinate basic ligands after activation.[47,48] A second cyclometalation in a *para* position relative to the first cyclometalation event results in the formation of bifunctional, bismetalated pincer complexes (Figure 2).[49–52] These pincer complexes can be activated by means of removing the fourth ligand, which is generally a halide atom, through the addition of a suitable silver salt (e.g., $AgBF_4$, AgOTf, $AgNO_3$). This addition leads to the abstraction of the halide atom by Ag^+ (precipitating AgX), which leaves a cationic complex with open coordination sites and noncoordinating counterions. Coordination of this open site to nitriles < pyridines < thioureas < phosphines forms a strong, chemo-reversible bond.

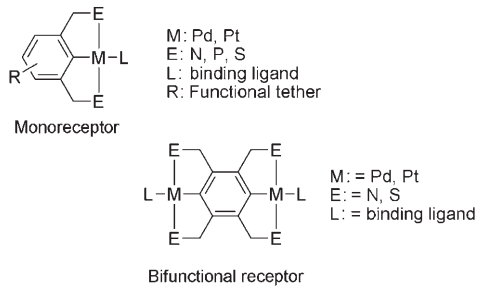

Figure 2. Examples of mono- and bismetallic pincer complexes as supramolecular synthons in which E is a neutral two-electron donor and L can be a functional recognition unit.

By using these four building blocks (**1**–**4**) we should be able to fine-tune the K_a values and ultimately the polymer properties. The K_a value of the metal–pyridyl-ligand interaction of each cruciform is expected to vary depending on the nature of the *para* substituent, which is an alkenyl group in **1** or an alkynyl group in **3**. This electronic effect has been shown to fit the Hammett equation by using the σ^+ constant[53] of the *para* substituent.[34] Furthermore, Pt pincer complexes have a significantly stronger association than Pd pincer complexes, which also allows us to control the association through the choice of the metal center.[54] Therefore, the uniqueness of each metal–ligand interaction within these structurally related supramolecular materials should lead to the formation of polymers with a set of properties that can be easily controlled.

Results and Discussion

Monomers **1**–**4** were synthesized by following literature procedures.[15,16,49,51,52] In **2** and **4**, acetonitrile molecules are coordinated to the metal centers of each respective pincer complex. The weaker coordination of the nitrile groups leads to a spontaneous and quantitative exchange of the acetonitrile molecules for the pyridyl-functionalized cruciform ligands to give polymers **1P**–**4P** in excellent yields. Self-assembly is accomplished by means of combining the bismetalated pincer complexes with the cruciform of choice. For solubility purposes, all of our physical characterization studies were carried out in DMF, except for fluorescence studies, which were performed in a $CHCl_3$/DMSO mixture.

By using ^{1}H NMR spectroscopy, the self-assembly process was monitored by changes in chemical shift of diagnostic signals pre- and post-coordination in [D_7]DMF. Both **2** and **4** showed shifts that are characteristic of quantitative metal-coordination events. The doublet at $\delta = 8.65$ ppm, which is representative of the α-pyridyl protons of cruciform **1**, showed a quantitative upfield shift to $\delta = 8.50$ ppm after coordination to **2** and a quantitative downfield shift to $\delta = 9.21$ ppm after coordination to **4**. In cruciform **3**, the α-pyridyl signal has an upfield shift from $\delta = 8.80$ to 8.63 ppm after coordination to **2**, and a downfield shift to $\delta = 9.35$ ppm after coordination to **4**.[55] We observed a broadening of all the signals for **1P**–**4P**, which is typical for polymers. As an example, Figure 3 shows the formation of **3P**, and the aromatic region of **1** before and after coordination to **4** in [D_7]DMF. The quantitative shifts of every proton along the distyryl axis are shown; protons further from the coordinated pyridyl nitrogen have smaller shifts because they experience less of an electronic perturbation. Additionally, the unaffected doublet of doublets labeled ***ε*** and ***ζ*** in the spectra shows the electronically decoupled nature of the cross-conjugated arylethynylene axis.

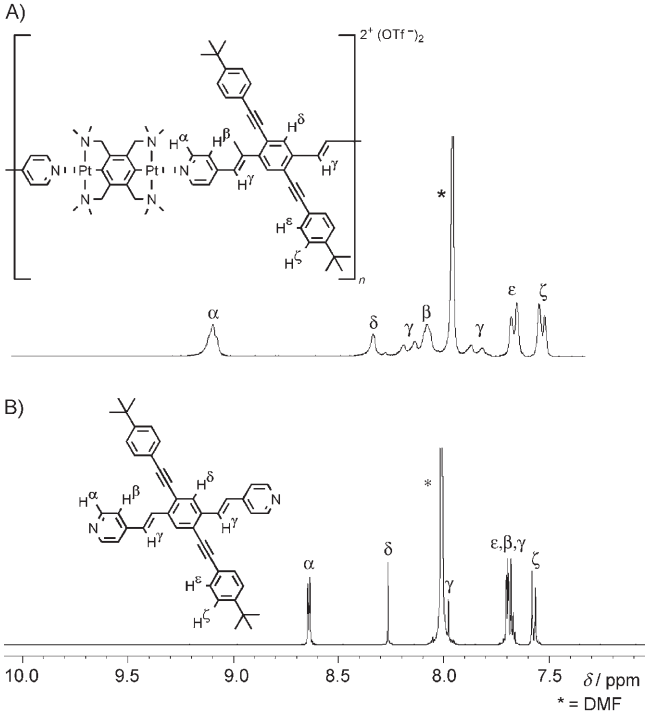

Figure 3. Stacked ^{1}H NMR spectra of the aromatic region in [D_7]DMF depicting the metal coordination of **1** to **4**. A) 1:1 mixture of **1**/**4** to give polymer **3P** (0.006 M) and B) cruciform **1** (0.006 M).

We quantified the strength of our metal–ligand interactions using ITC to provide complete thermodynamic characterization, which is calculated from the measured enthalpy of binding. For our experiments we assumed that the K_a value of our interaction is independent of the polymer length, that is, $K_{average} \approx K_1 \approx K_n$. By means of titrating a solution of each bismetalated pincer complex in DMF (10 mM) into a solution of each cruciform in DMF (1 mM) at 22 °C an isotherm is generated, from which a K_a ($K_{average}$) value is calculated. All titrations were carried out in triplicate to validate the reported K_a values. Furthermore, all isotherms showed a hyperbolic shape that is characteristic of a weak, dynamic on/off binding event, as presented in Figure 4 for the isotherm of **3P** (see Table 1).

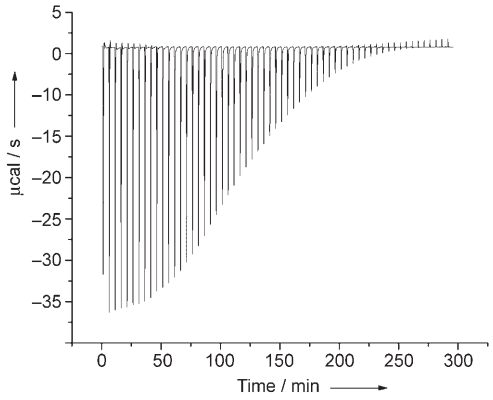

Figure 4. Isotherm generated from the titration of **4** into **1** in DMF to give **3P**.

Table 1. ITC K_a values and approximate degree of polymerization of each supramolecular complex.

	K_a [M^{-1}]	Maximum DP[a]
1P	$5.7(\pm1.6)\times10^3$	14
2P	$2.1(\pm0.5)\times10^3$	10
3P	$44.3(\pm5.4)\times10^3$	53
4P	$15.2(\pm2.9)\times10^3$	31
2·Pyr	$6.0(\pm0.5)\times10^3$	-
4·Pyr	$60.0(\pm7.8)\times10^3$	-
1·5	$9.8(\pm3.2)\times10^3$	-
1·6	$53.0(\pm4.8)\times10^3$	-

[a] Maximum DP $\approx (K_a[\text{monomer}])^{1/2}$, based on a 1:1 A/B supramolecular monomer concentration of 0.033 M in DMF.

The polymer K_a values were higher with **4** than with **2** by approximately an order of magnitude. Literature reports indicate that Pt-based coordination using pincer complexes is significantly stronger than using their palladium analogues,[54] which is in accordance with our results. The range of association strengths available for coordination events involving cruciforms can be used to control the properties of our system. However, the assumption that $K_a = K_{average}$ must first be validated. To this end, we carried out small-molecule binding studies for pincer complexes **2** and **4,** and cruciform **1**, in which the K_a values were measured and compared to K_a ($K_{average}$) values measured for the coordination polymer. For pincer complexes **2** and **4** we measured the K_a values upon the coordination of pyridine, and for cruciform **1** we measured the K_a values upon the coordination of monotopic Pd and Pt pincer complexes **5** and **6**, respectively, all in DMF.

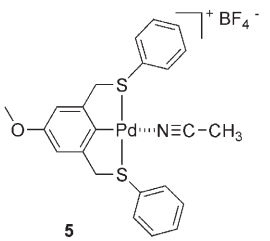

5

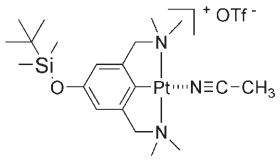

6

The close agreement of the small model K_a values to the polymeric K_a values strengthens the assumption that $K_a = K_{average}$ is valid. We obtain a set of DP values after inserting these K_a values into the MSOA model equation.

After confirming and quantifying the self-assembly of each of our systems by using ^{1}H NMR spectroscopy and ITC, we subsequently characterized the polymer properties. Owing to the weaker K_a values of our materials in DMF, size-exclusion chromatography was unreliable for determining the molecular weights and polydispersities of the polymers. Therefore, we analyzed the materials by viscometry by using a Cannon Ubbelohde semi-micro viscometer. Previously, we showed that there was a molecular-weight dependence of **1P** based on the monomer-feed ratios in DMF, with a maximum relative viscosity (η_r) with stoichiometric equivalences of **1** and **2**.[22] Under these conditions the longest possible length of the polymers in solution is obtained, when maximum coordination is assumed. Deviation from a 1:1 monomer-feed ratio led to chain termination and a less viscous solution as the length of the supramolecular polymer decreased.

Herein, we investigated the η_r values at different concentrations in DMF. A linear increase in η_r is generally expected as one increases the concentration of a covalent polymer solution. However, because our metal–ligand interactions are more favored at higher concentrations, a nonlinear increase should be observed. Figure 5 shows our viscometry results. The expected nonlinear increase is seen for all of our materials. Our viscosity measurements are also in accordance with the K_a values determined by ITC. The solution of **3P** is 70 times more viscous than pure DMF, and both bis-Pt-pincer-complexed polymeric solutions **3P** and **4P** are significantly more viscous than bis-Pd-pincer-complexed polymeric solutions **1P** and **2P**. Polymers **1P** and **3P** coordinate to the metal through the more electron-rich pyridyl groups on the distyryl axis and have a higher relative viscosity than the polymers formed from cruciform **3**, which coordinates along the less electron-releasing arylethynylene axis.

The viscosity results illustrate the inherent control over the polymer properties in our supramolecular system. By

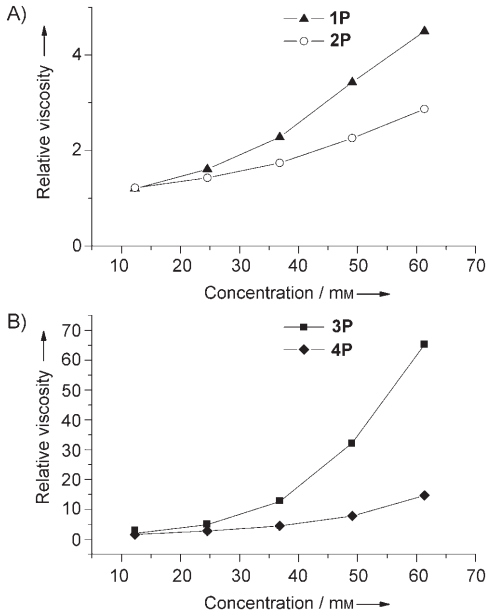

Figure 5. A) Plot of relative viscosity of bis-Pd pincer complexed materials **1P** and **2P**. B) Plot of relative viscosity of bis-Pt pincer complexed materials **3P** and **4P** in DMF.

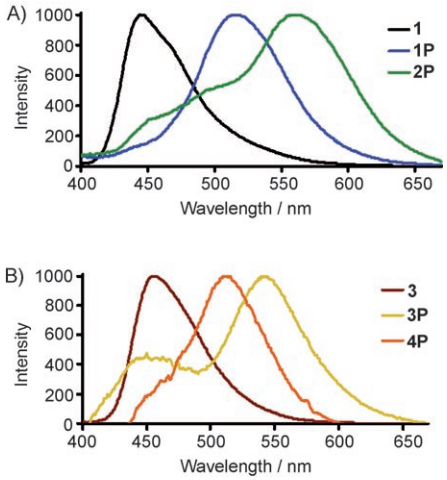

Figure 6. Normalized emission of cruciforms **1** and **3**, and λ_{max} of the furthest redshifted emissions of polymers **1P**–**4P** (precipitation seen at these maximum DPs) all at 0.0445 mM. A) Emission of cruciform **1** (black), and Pd coordination polymers **1P** (blue) and **3P** (green). B) Emission of cruciform **3** (maroon), and Pt coordination polymers **2P** (yellow) and **4P** (orange).

Table 2. Summary of the changes in emission (λ in nm) observed upon the addition of increasing numbers of equivalents of **2** or **4** to **1** or **3**. The concentration of the cruciform in all samples was 0.0445 mM in a mixture of $CHCl_3$/DMSO (95:5).

	Cruciform	Supramolecular complex[a]	Excess pincer[a]	Solid state
1P	445	515 (2.0)	485 (15.0)	520
2P	455	560 (3.6)	512 (20.0)	544
3P	445	542 (1.4)	–	–
4P	455	510 (3.0)	504 (15.0)	504

[a] Parentheses refer to the number of equivalents of ditopic pincer complex added to achieve shift.

Table 3. Summary of the changes in emission (λ in nm) observed upon the addition of **5** or **6** to **1** or **3**. The concentration of the cruciform in all samples was 0.0445 mM in a mixture of $CHCl_3$/DMSO (95:5).

	Cruciform	Supramolecular complex
1·5	445	491
3·5	455	507
1·6	445	540
3·6	455	515

simply switching one monomeric component with an alternate one from our supramolecular toolbox we can tune the DP, and thus the viscosity.

We examined the luminescent properties of these supramolecular materials. We used fluorescence spectroscopy to compare the emissions of **1P**–**4P** to that of their small-molecule analogues. Unlike the characterizations of our polymer physical properties, spectroscopic studies in DMF were not possible because the self-assembly was not readily observed at the dilute concentrations that were necessary for fluorescence measurements. As a result, we conducted all spectroscopic studies in a mixture of $CHCl_3$/DMSO (95:5).[56] For each supramolecular material we observed redshifted emissions relative to the uncoordinated cruciforms. We also observed a decrease in fluorescence intensity for each material proportional to the K_a values measured for each metal–ligand interaction. The results of this study are summarized in Figure 6 and Tables 2 and 3, with additional spectra included in the Supporting Information.

Uncoordinated **1** possesses a vibrant blue emission at $\lambda =$ 445 nm. Upon the titration of **2** (2.0 equiv), a bathochromic shift ($\lambda = 445 \rightarrow 515$ nm) is observed. If a large excess of **2** is added (15.0 equiv), a subsequent hypsochromic shift results ($\lambda = 515 \rightarrow 485$ nm). To rationalize these changes in emission, we performed a similar emission study in which monotopic Pd pincer complex **5** was coordinated to **1**. In the case of this model system, we observed a similar bathochromic shift ($\lambda = 445 \rightarrow 491$ nm) during the titration of **5**.

These emission shifts can be explained by the orthogonal arrangement of the FMOs in our cruciforms. Coordination in these cruciforms occurs along the LUMO axis. As corroborated from the ^{1}H NMR spectra, the HOMO axis is largely unaffected. Therefore, the LUMO is stabilized and the energy band-gap in all our systems decreases, which results in the bathochromic shifts observed.

This effect partially explains the change in emission observed upon the titration of **2** into **1**. During the early stages of the titration, coordination results in the assembly of polymer **1P** with an increasing DP. This putative high-molecular-weight material has limited solubility in the $CHCl_3$/DMSO mixture that was used for fluorescent measurements and led to aggregation, which was visually observed in the samples as clouding of the solution and formation of a precipitate. We have previously investigated cruciform aggregates in the

solid-state and observed differences in their emissive behavior.[18] We attribute the redshifted emission at $\lambda = 515$ nm for two equivalents of **2** to both LUMO stabilization and aggregation effects. This conclusion is further supported by the solid-state emission of **1P** at $\lambda = 520$ nm (dropcast film from a 1:2 mixture of **1**/**2**). However, upon the addition of an excess of pincer complex **2** (15 equiv), the formation of smaller end-capped oligomers, for example, **2·1·2** complexes, is favored. Unlike the highly charged polymer **1P**, these smaller species are soluble in $CHCl_3$, and therefore, the emission appears at a slightly lower wavelength ($\lambda = 485$ nm) than that of the initial uncoordinated cruciform. This emission is similar to the emission observed from the soluble model complex formed upon the addition of monotopic **5** to **1** ($\lambda = 491$ nm), which represents only the emission change from the stabilization of the LUMO after self-assembly.

We observed a similar trend for the self-assembly of **2P**, by detecting a bathochromic shift ($\lambda = 455 \rightarrow 560$ nm) during the initial stages of the titration of pincer complex **2** (3.6 equiv) into **3**. Further addition of **2** (20.0 equiv) resulted in a blueshift ($\lambda = 560 \rightarrow 512$ nm). Once again, we see a substantial bathochromic shift that results from complexation with **2**, as well as aggregation of the growing polymers; this results in a redshifted emission similar to that observed for **2P** in the solid state ($\lambda = 544$ nm). Addition of **2** (20 equiv) leads to the formation of soluble oligomers that emit at $\lambda =$ 512 nm, which is again is comparable to the emission observed upon the addition of monotopic **5** ($\lambda = 507$ nm) to **3**.

Changes in the optical properties of **1** and **3** are also observed upon assembly with bis-Pt pincer complex **4**. In the case of **3**, a bathochromic shift ($\lambda = 455 \rightarrow 510$ nm) is observed upon the addition of **4** (3.0 equiv). This emission is consistent with the solid-state emission observed at $\lambda =$ 504 nm. Further addition of **4** (15.0 equiv) results in a small blueshift ($\lambda = 510 \rightarrow 504$ nm) that corresponds to short-chain soluble oligomers. This emission is consistent with the emission observed for the model complex formed from cruciform **3** and monotopic Pt pincer **6** ($\lambda = 515$ nm). Assembly of **1** with **4** also resulted in a bathochromic shift ($\lambda = 445 \rightarrow$ 542 nm) upon the addition of **4** (1.4 equiv). However, further fluorescence measurements by using higher equivalents of pincer complex could not be made owing to near-baseline fluorescence intensity. Limited intensity also prevented us measuring the solid state-emission of **3P**.

The decrease in fluorescence intensity observed upon the self-assembly of each material also occurred in other cruciform coordination studies. Previously, we demonstrated that upon exposure to protons or metal cations, cruciforms **1** and **3** experience a sharp decrease in fluorescence quantum yield.[21] This effect is greater for protonation than for binding to metal cations, which suggests that a greater positive charge at the pyridine nitrogen results in a greater decrease in fluorescence intensity. We suggest that binding a proton or metal at the pyridyl nitrogen results in a stronger vibronic coupling between the ground and excited states, in addition to the heavy atom effect exerted by the Pt-pincer complex. Therefore, as binding increases then the nonradiative relaxation pathways from the excited state to the ground state become more accessible, which results in a decreased fluorescence intensity.

Conclusion

In summary, we have assembled four new supramolecular polymers by coordinating pyridyl-functionalized cruciforms **1** and **3** to either a ditopic bis-Pd or bis-Pt pincer complex. The fast and quantitative self-assembly process was characterized by ^{1}H NMR spectroscopy, and the association strength of each metal–ligand interaction was evaluated by using ITC. From these values, approximate degrees of polymerization were calculated. These data indicate that the pyridyl distyryl–Pt coordination is the strongest and the pyridyl ethynyl–Pd interaction is the weakest. The polymeric properties in solution were characterized by viscometry, the results from which complement the association strengths calculated from ITC, in which **3P** is the most viscous and **2P** is the least viscous solution. Finally, the luminescent properties of the polymers were measured by fluorescence spectroscopy. The emissions of the supramolecular materials were significantly redshifted from their uncoordinated cruciforms. The fluorescence intensity increased in the order **3P** < **1P** < **2P** < **4P**, and is inversely proportional to their association strength.

By developing, expanding, and studying the building blocks available for self-assembly, the strategy presented herein allows the design and synthesis of a class of novel functional organometallic polymers with predictable and tunable properties from a discrete set of monomers that circumvents problems associated with traditional covalent polymer synthesis. Each component in this system is amenable to further functionalization and modification to give us a virtually unlimited pool of monomers to investigate and exploit.

Future work in this area will focus on coordinating and investigating cruciforms with different substitution patterns to expand the physical and optical property ranges in the final polymers. Additionally, we will focus on improving the fluorescence quantum yields and solubility of the polymers through synthetic modifications to both monomeric constituents.

Experimental Section

General methods: All chemicals were purchased from Aldrich Chemical, Acros, or Fisher Scientific and used as received, unless otherwise specified. NMR spectra were recorded at 298 K by using a Varian Mercury spectrometer (300 MHz) and the residual solvent was used as an internal standard.

General procedures for ITC characterization of coordination complexes: All measurements were made by using a Microcal VP-ITC Microcalorimeter at 22 °C in anhydrous DMF that was degassed under reduced pressure.

Bis-metalated pincer complex–cruciform: The bismetalated pincer complex in DMF (10 mM) was titrated (5 μL injections over 10 s followed by an equilibration period) into a solution of the cruciform in DMF (1 mM). A reference run of each bismetalated-pincer-complex solution titrated into pure DMF was subtracted from each measurement to account for the heat of dilution. Each experiment was carried out in triplicate to validate all K_a values.

Monotopic pincer complex–cruciform: The monotopic-metalated pincer complex in DMF (20 mM) was titrated (5 μL injections over 10 s followed by an equilibration period) into a solution of the cruciform in DMF (1 mM). A reference run of each monotopic-metalated-pincer-complex solution titrated into pure DMF was subtracted from each measurement to account for the heat of dilution. Each experiment was carried out in triplicate to validate all K_a values. The reverse addition was also carried out to corroborate the data by means of titrating a cruciform solution in DMF (10 mM) into a monotopic-metalated-pincer-complex solution in DMF (1 mM) under identical conditions.

Bis-metalated pincer complex–pyridine: The bismetalated-pincer-complex solution in DMF (10 mM) was titrated (5 μL injections over 10 s followed by an equilibration period) into a solution of anhydrous pyridine in DMF (1 mM). A reference run of each bismetalated-pincer-complex solution titrated into pure DMF was subtracted from each measurement to account for the heat of dilution. Each experiment was carried out in triplicate to validate all K_a values. The reverse addition was also carried out to corroborate the data by means of titrating an anhydrous solution of pyridine in DMF (20 mM) into a solution of bismetalated pincer complex in DMF (1 mM) under identical conditions.

Viscometry: All studies were carried out in HPLC grade DMF by using a Cannon Ubbelohde semi-micro viscometer (No. 100 L182), and the time was measured by using a stopwatch at 25 °C. Initial solutions of each supramolecular material (0.033 mM) at a 1:1 stoichiometric ratio were prepared by dissolving each component (0.033 mmol) in DMF (1 mL) in the viscometer, sonicating the sample for 10 min, incubating it for 10 min, and then acquiring three efflux times. The solution within the viscometer was then diluted to 0.025, 0.018, 0.012, and 0.006 mM; between each measurement of these concentrations the solutions were equilibrated and the efflux times measured in triplicate.

Optical spectra: All samples were prepared by using spectroscopic grade solvents purchased from OmniSolv. All fluorescence spectra were recorded by a Shimadzu RF-5301PC spectrofluorophotometer and measured in a triangular quartz cuvette to minimize spectral artifacts (specifically self-absorption). Solutions were mixed (as specified in the Supporting Information) such that the final concentration of cruciform in all samples measured was 0.0445 mM in a mixture of $CHCl_3$/DMSO (95:5). All solution volumes were measured by using Eppendorf Reference variable-volume pipettes. Significant noise was present as a result of near-baseline fluorescence intensity in some cases. In addition, scattering peaks were present. A spectrum of the triangular cuvette filled with solvent was recorded and subtracted to minimize scattering artifacts. Corrected and uncorrected spectra are included in the Supporting Information. In addition, emission spectra were normalized to highlight the observed shifts.

Solid-state emission spectra: Solid-state emission spectra were obtained for **1P**, **2P**, and **4P** (spectra for **3P** could not be obtained owing to baseline fluorescence intensity). Solutions were dropcast onto glass slides and dried under a flow of air. Emission spectra were acquired by using a Shimadzu RF-5301PC spectrofluorophotometer. The spectra of the glass slides were subtracted to remove minor scattering effects. Uncorrected and corrected spectra are included in the Supporting Information.

Solution photographs: Photographs of the solutions used for optical measurements were taken to qualitatively demonstrate the changes in fluorescence observed upon assembly. The concentration of cruciform in all samples measured was 0.0445 mM in a mixture of $CHCl_3$/DMSO (95:5). Photographs were taken under illumination at 365 nm by using a Canon EOS 30D digital camera equipped with a Canon EFS 18–55 mm zoom lens.

Acknowledgements

Financial support has been provided by the National Science Foundation (CHE-0239385 and DMR-0454471). M.W. acknowledges a DuPont Young Professor Award, an Alfred P. Sloan Fellowship, and a Camille Dreyfus Teacher/Scholar Award.

[1] *Electronic Materials: The Oligomer Approach*, (Eds.: G. Wegner, K. Müllen), Wiley-VCH, Weinheim, **1996**.
[2] A. Kraft, A. C. Grimsdale, A. B. Holmes, *Angew. Chem.* **1998**, *110*, 416–443; *Angew. Chem. Int. Ed.* **1998**, *37*, 402–428.
[3] C. D. Dimitrakopoulos, P. R. L. Malenfant, *Adv. Mater.* **2002**, *14*, 99–117.
[4] U. Mitschke, P. Bäuerle, *J. Mater. Chem.* **2000**, *10*, 1471–1507.
[5] Y. Shirota, *J. Mater. Chem.* **2000**, *10*, 1–25.
[6] R. D. McCullough, *Adv. Mater.* **1998**, *10*, 93–116.
[7] R. H. Friend, R. W. Gymer, A. B. Holmes, J. H. Burroughes, R. N. Marks, C. Taliani, D. D. C. Bradley, D. A. Dos Santos, J. L. Brédas, M. Lögdlund, W. R. Salaneck, *Nature* **1999**, *397*, 121–128.
[8] R. Dobrawa, M. Lysetska, P. Ballester, M. Grüne, F. Würthner, *Macromolecules* **2005**, *38*, 1315–1325.
[9] P. Y. W. Dankers, M. C. Harmsen, L. A. Brouwer, M. J. A. Van Luyn, E. W. Meijer, *Nat. Mater.* **2005**, *4*, 568–574.
[10] M. H. Chang, F. J. M. Hoeben, P. Jonkheijm, A. P. H. J. Schenning, E. W. Meijer, C. Silva, L. M. Herz, *Chem. Phys. Lett.* **2006**, *418*, 196–201.
[11] P. K. Iyer, J. B. Beck, C. Weder, S. J. Rowan, *Chem. Commun.* **2005**, 319–321.
[12] D. Knapton, S. J. Rowan, C. Weder, *Macromolecules* **2006**, *39*, 651–657.
[13] J. B. Beck, J. M. Ineman, S. J. Rowan, *Macromolecules* **2005**, *38*, 5060–5068.
[14] A. Kokil, P. Yao, C. Weder, *Macromolecules* **2005**, *38*, 3800–3807.
[15] J. N. Wilson, M. Josowicz, Y. Wang, U. H. F. Bunz, *Chem. Commun.* **2003**, 2962–2963.
[16] J. N. Wilson, U. H. F. Bunz, *J. Am. Chem. Soc.* **2005**, *127*, 4124–4125.
[17] J. N. Wilson, K. I. Hardcastle, M. Josowicz, U. H. F. Bunz, *Tetrahedron* **2004**, *60*, 7157–7167.
[18] J. N. Wilson, M. D. Smith, V. Enkelmann, U. H. F. Bunz, *Chem. Commun.* **2004**, 1700–1701.
[19] D. M. Ciurtin, N. G. Pschirer, M. D. Smith, U. H. F. Bunz, H.-C. zur Loye, *Chem. Mater.* **2001**, *13*, 2743–2745.
[20] J. N. Wilson, P. M. Windscheif, U. Evans, M. L. Myrick, U. H. F. Bunz, *Macromolecules* **2002**, *35*, 8681–8683.
[21] A. J. Zucchero, J. N. Wilson, U. H. F. Bunz, *J. Am. Chem. Soc.* **2006**, *128*, 11872–11881.
[22] W. W. Gerhardt, A. J. Zucchero, J. N. Wilson, C. R. South, U. H. F. Bunz, M. Weck, *Chem. Commun.* **2006**, 2141–2143.
[23] $DP \approx (K[\text{monomer}])^{1/2}$.
[24] A. Ciferri, *Macromol. Rapid Commun.* **2002**, *23*, 511–529.
[25] R. Dobrawa, F. Würthner, *J. Polym. Sci., Part A: Polym. Chem.* **2005**, *43*, 4981–4995.
[26] J. A. Marsden, J. J. Miller, L. D. Shirtcliff, M. M. Haley, *J. Am. Chem. Soc.* **2005**, *127*, 2464–2476.
[27] J. E. Klare, G. S. Tulevski, K. Sugo, A. de Picciotto, K. A. White, C. Nuckolls, *J. Am. Chem. Soc.* **2003**, *125*, 6030–6031.
[28] J. E. Klare, G. S. Tulevski, C. Nuckolls, *Langmuir* **2004**, *20*, 10068–10072.
[29] H. Kang, P. Zhu, Y. Yang, A. Facchetti, T. J. Marks, *J. Am. Chem. Soc.* **2004**, *126*, 15974–15975.
[30] H. Kang, G. Evmenenko, P. Dutta, K. Clays, K. Song, T. J. Marks, *J. Am. Chem. Soc.* **2006**, *128*, 6194–6205.
[31] J. K. Sørensen, M. Vestergaard, A. Kadziola, K. Kilså, M. B. Nielsen, *Org. Lett.* **2006**, *8*, 1173–1176.
[32] H.-Y. Wang, J.-C. Feng, G.-A. Wen, H.-J. Jiang, J.-H. Wan, R. Zhu, C.-M. Wang, W. Wei, W. Huang, *New J. Chem.* **2006**, *30*, 667–670.
[33] Z. H. Li, M. S. Wong, Y. Tao, *Tetrahedron* **2005**, *61*, 5277–5285.

[34] H.-J. van Manen, K. Nakashima, S. Shinkai, H. Kooijman, A. L. Spek, F. C. J. M. van Veggel, D. N. Reinhoudt, *Eur. J. Inorg. Chem.* **2000**, 2533–2540.
[35] J. M. Pollino, L. P. Stubbs, M. Weck, *J. Am. Chem. Soc.* **2004**, *126*, 563–567.
[36] J. M. Pollino, M. Weck, *Synthesis* **2002**, 1277–1285.
[37] J. M. Pollino, M. Weck, *Org. Lett.* **2002**, *4*, 753–756.
[38] M. N. Higley, J. M. Pollino, E. Hollembeak, M. Weck, *Chem. Eur. J.* **2005**, *11*, 2946–2953.
[39] W. T. S. Huck, F. C. J. M. van Veggel, D. N. Reinhoudt, *J. Mater. Chem.* **1997**, *7*, 1213–1219.
[40] W. T. S. Huck, L. J. Prins, R. H. Fokkens, N. M. M. Nibbering, F. C. J. M. van Veggel, D. N. Reinhoudt, *J. Am. Chem. Soc.* **1998**, *120*, 6240–6246.
[41] S.-E. Stiriba, M. Q. Slagt, H. Kautz, R. J. M. K. Gebbink, R. Thomann, H. Frey, G. van Koten, *Chem. Eur. J.* **2004**, *10*, 1267–1273.
[42] F. R. Kersey, W. C. Yount, S. L. Craig, *J. Am. Chem. Soc.* **2006**, *128*, 3886–3887.
[43] A. Friggeri, H.-J. van Manen, T. Auletta, X.-M. Li, S. Zapotoczny, H. Schönherr, G. J. Vancso, J. Huskens, F. C. J. M. van Veggel, D. N. Reinhoudt, *J. Am. Chem. Soc.* **2001**, *123*, 6388–6395.
[44] W. W. Gerhardt, M. Weck, *J. Org. Chem.* **2006**, *71*, 6333–6341.
[45] G. Guillena, G. Rodríguez, M. Albrecht, G. van Koten, *Chem. Eur. J.* **2002**, *8*, 5368–5376.
[46] G. Guillena, G. Rodríguez, G. van Koten, *Tetrahedron Lett.* **2002**, *43*, 3895–3898.
[47] M. Albrecht, G. van Koten, *Angew. Chem.* **2001**, *113*, 3866–3898; *Angew. Chem. Int. Ed.* **2001**, *40*, 3750–3781.
[48] M. Q. Slagt, G. Rodríguez, M. M. P. Grutters, R. J. M. K. Gebbink, W. Klopper, L. W. Jenneskens, M. Lutz, A. L. Spek, G. van Koten, *Chem. Eur. J.* **2004**, *10*, 1331–1344.
[49] S. J. Loeb, G. K. H. Shimizu, *J. Chem. Soc. Chem. Commun.* **1993**, 1395–1397.
[50] S. J. Loeb, G. K. H. Shimizu, J. A. Wisner, *Organometallics* **1998**, *17*, 2324–2327.
[51] P. Steenwinkel, S. L. James, D. M. Grove, H. Kooijman, A. L. Spek, G. van Koten, *Organometallics* **1997**, *16*, 513–515.
[52] P. Steenwinkel, H. Kooijman, W. J. J. Smeets, A. L. Spek, D. M. Grove, G. van Koten, *Organometallics* **1998**, *17*, 5411–5426.
[53] H. C. Brown, Y. Okamoto, *J. Am. Chem. Soc.* **1958**, *80*, 4979–4987.
[54] W. C. Yount, D. M. Loveless, S. L. Craig, *J. Am. Chem. Soc.* **2005**, *127*, 14488–14496.
[55] The directionally opposite shift of the α-pyridyl cruciform signal observed in the ^{1}H NMR spectrum upon coordination to the bis-Pd pincer complex **2** relative to the shift after coordination to the bis-Pt pincer complex **4** is a result of an overlap of the pyridyl protons with the thiophenyl ring currents of bis-Pd pincer complex **2**, see ref. [34].
[56] Owing to the highly dilute $CHCl_3$/DMSO solvent mixture we did not observe the expected polymerization at a metal/ligand stoichiometry of 1:1. Putative high-molecular-weight polymers, which precipitated out of solution were not seen until an excess of the pincer complex was titrated into the cruciform solution. As the K_a value increased, precipitation of the respective complex occurred closer to the expected 1:1 stoichiometry.

Received: November 10, 2006
Published online: March 8, 2007

